The Plant Cell, Vol. 25: 1078–1092, March 2013, www.plantcell.org

Modularity of Plant Metabolic Gene Clusters: A Trio of Linked Genes That Are Collectively Required for Acylation of Triterpenes in Oat[W][OA]

Sam T. Mugford,[a] Thomas Louveau,[a] Rachel Melton,[a] Xiaoquan Qi,[a,1] Saleha Bakht,[a] Lionel Hill,[a] Tetsu Tsurushima,[a,b] Suvi Honkanen,[a,c] Susan J. Rosser,[c] George P. Lomonossoff,[a] and Anne Osbourn[a,2]

[a] John Innes Centre, Norwich NR4 7UH, United Kingdom
[b] Faculty of Business, Han-nan University, Matsubara City, Osaka 580, Japan
[c] Institute of Molecular Cell and Systems Biology, University of Glasgow, Glasgow G12 8QQ, United Kingdom

Operon-like gene clusters are an emerging phenomenon in the field of plant natural products. The genes encoding some of the best-characterized plant secondary metabolite biosynthetic pathways are scattered across plant genomes. However, an increasing number of gene clusters encoding the synthesis of diverse natural products have recently been reported in plant genomes. These clusters have arisen through the neo-functionalization and relocation of existing genes within the genome, and not by horizontal gene transfer from microbes. The reasons for clustering are not yet clear, although this form of gene organization is likely to facilitate co-inheritance and co-regulation. Oats (*Avena* spp) synthesize antimicrobial triterpenoids (avenacins) that provide protection against disease. The synthesis of these compounds is encoded by a gene cluster. Here we show that a module of three adjacent genes within the wider biosynthetic gene cluster is required for avenacin acylation. Through the characterization of these genes and their encoded proteins we present a model of the subcellular organization of triterpenoid biosynthesis.

INTRODUCTION

Plants synthesize a diverse range of specialized metabolites (also commonly referred to as natural products), many of which have important roles in protection against disease, herbivory, and/or abiotic stress (Dixon, 2001; Osbourn and Lanzotti 2009). Oats (*Avena* spp) produce antimicrobial triterpene glycosides (avenacins) in their roots that protect against soil-borne pathogens (Hostettmann and Marston, 1995; Papadopoulou et al., 1999; Osbourn et al., 2011). Although a diverse array of structurally varied triterpene glycosides is found in dicots, the ability to synthesize glycosylated triterpenes is rare in the cereals and grasses. Avenacins exhibit some unusual structural features that are not shared by other plant triterpene glycosides. Most notably, they are acylated at the carbon-21 (C-21) position with either *N*-methyl anthranilate or benzoate (Figure 1). A recent review of structure-function relationships in triterpenoids indicates that C-21 acylation is important in determining the biological activity of some triterpenes (Podolak et al., 2010). Understanding the mechanisms underlying this type of modification has potential to provide powerful biotechnological tools for the modification of triterpene structure and function in different biological systems.

Acylation orchestrates the amalgamation of complex chemical groups with different biochemical origins into single compounds and so offers great versatility in modulating the form and function of plant natural products (D'Auria, 2006). Plant acyltransferase enzymes have been identified that catalyze the transfer of a wide range of acyl groups onto a diverse set of acceptor substrates belonging to different classes of natural product. These enzymes belong to two unrelated families: the BAHD acyltransferases, which use CoA-thioesters as the acyl donor (Yang et al., 1997; Dudareva et al., 1998; Fujiwara et al., 1998; St-Pierre et al., 1998; Walker et al., 2002; Luo et al., 2007, 2009; Grienenberger et al., 2009); and the serine carboxypeptidase-like (SCPL) acyltransferases, which use *O*-Glc esters as acyl donors. The SCPL-acyltransferases belong to the serine carboxypeptidase family but have acquired different functions to these ancestral proteases (Lehfeldt et al., 2000; Li and Steffens, 2000; Shirley et al., 2001; Fraser et al., 2007; Weier et al., 2008; Shirley and Chapple, 2003; Milkowski and Strack, 2004; Milkowski et al., 2004; Baumert et al., 2005; Stehle et al., 2008; Mugford et al., 2009; Mugford and Osbourn, 2010; Mugford and Milkowski, 2012). Based on the available evidence, it seems likely that the two different families of acyltransferases are also distinguished by their subcellular localizations. The *Arabidopsis thaliana* sinapoyl-malate SCPL-acyltransferase SMT has been localized to the vacuole (Hause et al., 2002), and other members of this family are likewise predicted to be targeted to the vacuole in *Arabidopsis* and other plants (Fraser et al., 2005). Conversely, members of the BAHD family have either been shown to be or are predicted to be cytosolic (Fujiwara et al., 1998; D'Auria, 2006; Yu et al., 2008).

We previously established a collection of avenacin-deficient mutants of the diploid oat species *Avena strigosa*. The major

[1] Current address: Institute of Botany, Chinese Academy of Sciences, Nanxincun 20, Fragrance Hill, Beijing 100093, China.
[2] Address correspondence to anne.osbourn@jic.ac.uk.
The author responsible for distribution of materials integral to the findings presented in this article in accordance with the policy described in the Instructions for Authors (www.plantcell.org) is: Anne Osbourn (anne.osbourn@jic.ac.uk).
[W] Online version contains Web-only data.
[OA] Open Access articles can be viewed online without a subscription.
www.plantcell.org/cgi/doi/10.1105/tpc.113.110551

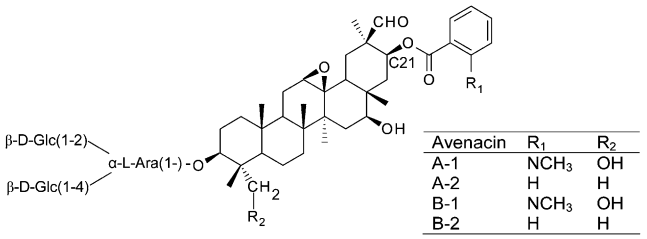

Avenacin	R_1	R_2
A-1	NCH_3	OH
A-2	H	H
B-1	NCH_3	OH
B-2	H	H

Figure 1. Structures of Oat Root Avenacins.

The C-21 acyl group consists of either *N*-methyl anthranilate or benzoate, depending on the R_1 group. The major avenacin found in oat roots is avenacin A-1, which is acylated with *N*-methyl anthranilate (Crombie et al., 1984).

avenacin, A-1, is esterified with *N*- methyl anthranilate and fluoresces strongly under ultraviolet illumination. Avenacin-deficient mutants of *A. strigosa* were isolated following sodium azide mutagenesis, using a simple screen for loss of root fluorescence. These avenacin-deficient mutants were found to have increased susceptibility to infection by soil-borne pathogens (Papadopoulou et al., 1999). This mutant collection has proved to be a valuable resource for investigating triterpenoid biosynthesis, and we cloned genes encoding several steps of the avenacin biosynthetic pathway (Haralampidis et al., 2001; Qi et al., 2004, 2006; Mugford et al., 2009; Owatworakit et al., 2012). An important discovery has been that the loci for the synthesis of avenacins are clustered. Although genes encoding plant metabolic pathways are generally regarded as randomly distributed in the genome, a growing number of plant natural product biosynthetic pathways have been identified that are encoded by operon-like gene clusters in plants (Frey et al., 1997; Gierl and Frey, 2001; Qi et al., 2004; Wilderman et al., 2004; Shimura et al., 2007; Field and Osbourn, 2008; Swaminathan et al., 2009; Chu et al., 2011; Falara et al., 2011; Field et al., 2011; Takos et al., 2011; Kliebenstein and Osbourn, 2012; Winzer et al., 2012).

We recently showed that an SCPL acyltransferase, SCPL1, is responsible for the acylation of avenacins in *A. strigosa* (Mugford et al., 2009). SCPL1 is encoded by *Sad7*, which forms part of the avenacin gene cluster. This enzyme catalyzes the transfer of *N*-methyl anthranilate from an *O*-Glc ester onto triterpenoid backbones to produce avenacins A-1 and B-1. It is also required for the formation of the two benzoylated forms of avenacin, A-2 and B-2 (Figure 1). In *Arabidopsis* and *Brassica* species, the glucosylated acyl donor substrates of SCPL acyltransferases are synthesized by family 1 glucosyltransferases (Lim et al., 2001; Baumert et al., 2005). We recently identified a family 1 glycosyltransferase (UGT74H5) in *A. strigosa* that catalyzes the glucosylation of *N*-methyl anthranilate to *N*-methyl anthranilate-*O*-Glc, the acyl donor substrate for SCPL1. UGT74H5 is encoded by the *A. strigosa Sad10* gene, which lies within the avenacin gene cluster, adjacent to the *Sad7* (*SCPL1*) gene (Owatworakit et al., 2012).

Here, we characterize a gene encoding an anthranilate *N*-methyltransferase (MT1, encoded by *Sad9*) and show that this enzyme acts together with the UGT74H5 glucosyltransferase and the SCPL1 acyltransferase in the final steps of the synthesis of avenacin A-1. These three genes are adjacent within the wider avenacin biosynthetic gene cluster and so represent an acylation module. We present evidence that acylation of avenacins is important for the potent biological activity of these molecules. This three-gene cassette may therefore be a useful resource for the heterologous modification of triterpenes with altered biological activity. By combining biochemical and genetic approaches with investigation of the subcellular localization of the enzymes of avenacin biosynthesis, we further establish a model for the spatial organization of triterpenoid synthesis.

RESULTS

Three Genes Encoding a Methyltransferase, Glucosyltransferase, and an Acyltransferase Are Adjacent within the Avenacin Gene Cluster

Previously, we identified and sequenced a BAC contig spanning four genes within the avenacin gene cluster: *Sad1*, *2*, *7*, and *10* (Qi et al., 2006; Mugford et al., 2009; Owatworakit et al., 2012). Further extension of this BAC contig identified a gene predicted to encode an *S*-adenosyl-methionine–dependent methyltransferase (MT1), which lies 45 kb from the *UGT74H5* (*Sad10*) gene (Figure 2A). Avenacins A-1 and B-1 are both acylated with *N*-methyl anthranilate, implicating anthranilate methylation in the avenacin biosynthetic pathway. Phylogenetic analysis shows that MT1 lies within a clade of methyltransferases that consists mainly of *O*-methyltransferase enzymes with roles in secondary metabolism (Figure 2B; see Supplemental Data Set 1 online), although two characterized members of this clade (*Limonium latifolium* β-alanine-*N*-methyltransferase and *Ruta graveolens* anthranilate-*N*-methyltransferase) are known to have *N*-methyltransferase activity (Liscombe and Facchini, 2007; Rohde et al., 2008), consistent with a possible role for MT1 as an *N*-methyltransferase. Avenacins are synthesized in the epidermal cells of the root tip, and the expression of genes that encode the previously characterized steps in the biosynthetic pathway is restricted to these cells (Qi et al., 2006; Wegel et al., 2009; Mugford et al., 2009). Quantitative PCR analysis revealed that the *MT1* transcript is most abundant in whole root and root tip samples, low in the upper root, and not detectable in young leaves (Figure 2C). Immunoblot analysis detected MT1 in extracts from the roots but not the leaves of wild-type *A. strigosa* seedlings, as is the case for other avenacin biosynthetic enzymes (Figure 3, lanes 1 and 2). Furthermore, immunostaining of root tip tissue sections with specific antisera raised against As-MT1 indicates that the protein is restricted to the epidermal cells of the root tip (Figure 2D). A similar pattern of staining is also observed using antisera raised against the As-SCPL1 protein. Signals were not observed for sections stained with the corresponding preimmune sera (see Supplemental Figure 1 online). Collectively, these results are consistent with a role for As-MT1 in avenacin biosynthesis.

MT1 Is Required for *N*-Methylation of Avenacin A-1 and Corresponds to *Sad9*, a Locus Previously Defined by Mutation

We previously isolated a collection of avenacin-deficient mutants of *A. strigosa* that were identified from a screen for loss of UV fluorescence in the root tip (Papadopoulou et al., 1999; Qi et al.,

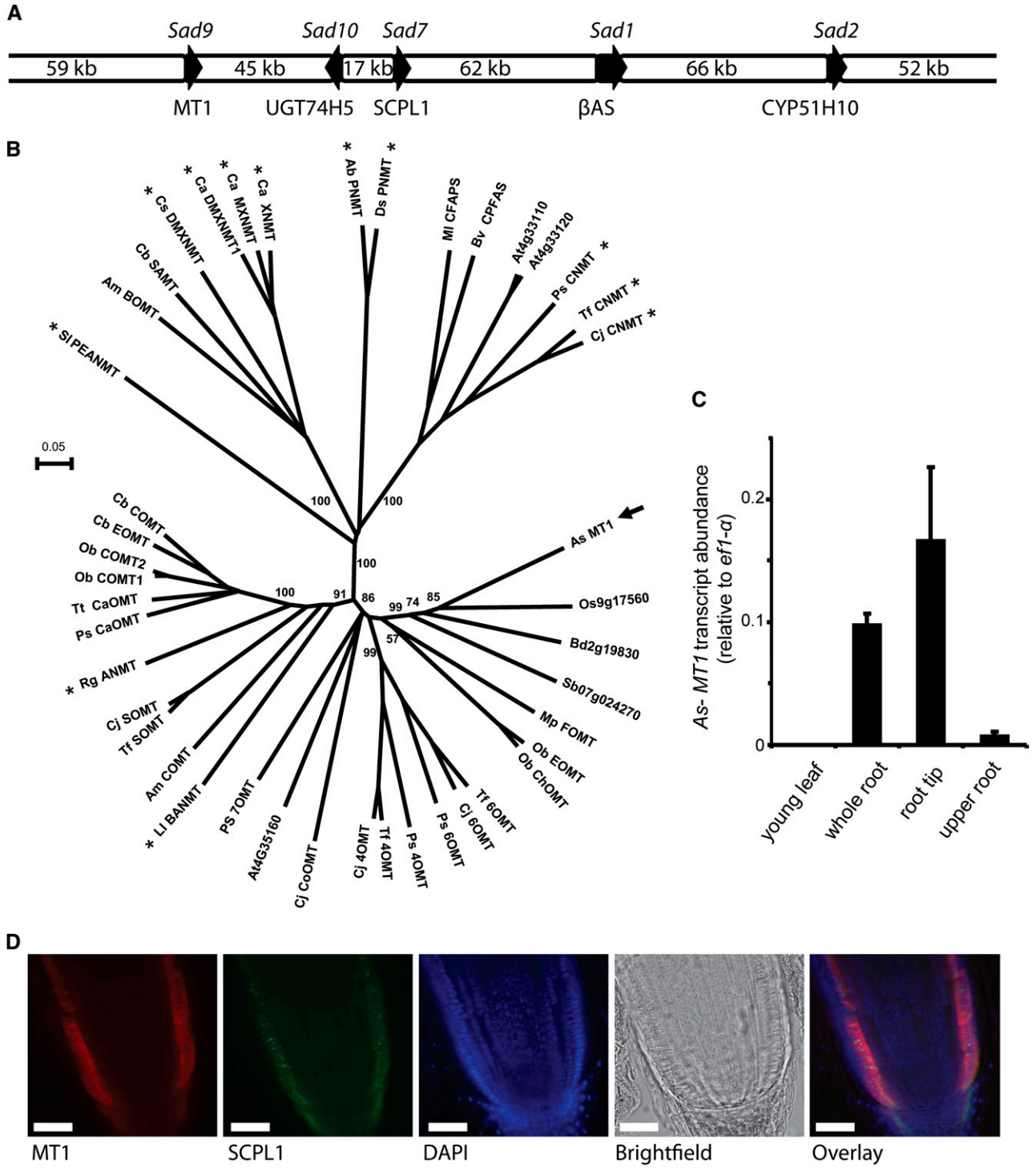

Figure 2. A Gene Encoding a Predicted Methyltransferase Located within the Avenacin Biosynthetic Gene Cluster Is Implicated in Avenacin Synthesis.

(A) BAC contig showing the avenacin gene cluster and the location of the *Sad9* gene, which is predicted to encode a methyltransferase. Gene names are indicated above and encoded proteins below.

(B) Neighbor-joining phylogeny of functionally characterized plant natural product *S*-adenosyl-Met–dependent methyltransferase enzymes. *N*-methyltransferase enzymes are indicated with asterisks. The phylogeny includes the sequences used by Liscombe and Facchini, 2007; the MT1 protein (indicated by an arrow); the most similar sequences to As-MT1 encoded by the genomes of *Arabidopsis* (At4g35160), rice (*Oryza sativa*; Os9g17560), *Brachypodium distachyon* (Bd2g19830), and sorghum (*Sorghum bicolor*; Sb07g024270); and the *R. graveolens* anthranilate methyltransferase (Rg

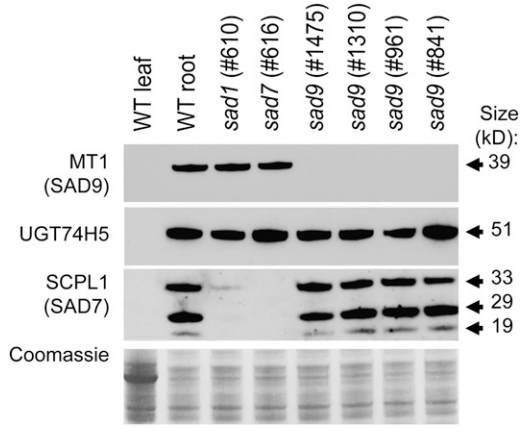

Figure 3. Detection of MT1, UGT74H5, and SCPL1 in Oat Roots.

Immunoblot analysis of soluble protein extracts from 3-d-old *A. strigosa* seedlings, probed with antisera raised against MT1, UGT74H5, or SCPL1. The bottom panel shows Coomassie blue staining of a replicate gel. Protein extracts were prepared from leaves and roots of 3-d-old *A. strigosa* wild-type (WT) seedlings and from roots of previously characterized *sad1* (mutant line #610) and *sad7* (#616) mutants (Papadopoulou et al., 1999; Mugford et al., 2009) and *sad9* mutants (#1475, 1310, 961, and 841) (this article). Bands corresponding to the predicted size of the MT1 and UGT74H5 proteins were detected. SCPL1 is posttranslationally cleaved into a large and a small subunit corresponding to the bands detected at 29 and 19 kD and a processing intermediate (33 kD) (Mugford et al., 2009).

2006). Liquid chromatography–mass spectrometry (LC-MS) analysis of this mutant collection identified four independent mutants that lacked avenacin A-1 but accumulated a related compound that is acylated with anthranilate rather than *N*-methyl anthranilate (des-methyl avenacin A-1 [DMA]) (Figure 4A; see Supplemental Figure 2 online). These four mutant lines (#1475, #1310, #961, and #841) were shown to be allelic. The roots of early avenacin pathway mutants (*sad1* and *sad2*) (Papadopoulou et al., 1999; Qi et al., 2004, 2006; Qin et al., 2010) have little or no fluorescence, while those of *sad7* have weak blue autofluorescence due to the accumulation of the acyl donor *N*-methyl anthraniloyl-*O*-Glc (Mugford et al., 2009). By contrast, roots of *sad9* mutants have a weak purple fluorescence under UV illumination. The fluorescence of extracts from wild-type roots peaks at 440 nm compared with 410 nm from the *sad9* mutant. This is consistent with the fluorescence of *N*-methyl anthranilate (blue) compared with that of anthranilate (purple). LC-MS analysis revealed that DMA is found not only in *sad9* mutants, but also in wild-type *A. strigosa* roots (Figure 4). *sad9* mutants lack *N*-methyl anthraniloyl-*O*-Glc but accumulate a fluorescent compound with mass spectrum and fragmentation pattern consistent with anthraniloyl-*O*-glucose (Figure 4A; see Supplemental Figure 2 online). Quantification of acylated avenacins in a selection of mutants showed that DMA accumulates in the *sad9* mutants at lower levels (109.0 ± 29.9 pmol/mg fresh weight in #961; 189.2 ± 26.5 pmol/mg fresh weight in #1310) than is found for avenacin A-1 in the wild type (365.3 ± 8.9 pmol/mg fresh weight) (values are means of four replicate samples ± SE). In addition, the *sad9* mutants accumulate des-acyl avenacin, which is also found in the *sad7* mutants (Figure 4), and the nonfluorescent avenacins A-2 and B-2, which are acylated with benzoate and are also present at similar levels in the wild type (see Supplemental Table 1 online).

The failure of *sad9* mutants to methylate avenacin and the presence of *MT1* (encoding a predicted methyltransferase) in the avenacin gene cluster suggests that *Sad9* and *MT1* may be synonymous. DNA sequence analysis of *MT1* in the *sad9* mutants revealed nonsynonymous point mutations in all four alleles (#841, C998T and A333V; #961, C89T and S30F; #1310, G978A and W326Stop; #1475, C235T and R79W) that alter single amino acids or in the case of #1310 introduce a stop codon, indicating that *Sad9* is likely to encode MT1. These data suggest a pathway for acylation of avenacin as shown in Figure 4B that involves *N*-methylation of anthranilate by MT1 (SAD9), glucosylation of *N*-methyl anthranilate by UGT74H5 (SAD10), and the transfer of the acyl group to the triterpene backbone by SCPL1 (SAD7). In the absence of MT1, SCPL1 is apparently still able to acylate avenacins using anthraniloyl-*O*-Glc as the acyl donor instead of *N*-methyl anthraniloyl-*O*-Glc.

Previously we have shown that *sad1*, *sad2*, and *sad7* mutants of *A. strigosa* have increased susceptibility to soil-borne fungal pathogens (Papadopoulou et al., 1999; Qi et al., 2004, 2006; Mugford et al., 2009). Pathogenicity tests with *Gaeumannomyces graminis* var *tritici*, the causal agent of take-all disease of cereals, revealed that, like *sad1*, *sad2*, and *sad7* mutants, *sad9* mutants are more susceptible to infection than wild-type seedlings (Figure 5). The increased susceptibility of *sad7* and *sad9* mutants to disease may be because correct acylation of avenacins is required for antifungal activity or, alternatively, because the unacylated/incorrectly acylated avenacins accumulate at lower levels in the mutants. We measured the total concentrations of avenacins and des-acyl avenacins in wild-type and *sad7* mutant oat roots and found that the levels of unacylated avenacins in the *sad7* mutant roots were comparable to the levels of acylated avenacins in the wild type (see Supplemental Figure 3 online), indicating that the acyl group is likely to be important in protecting against disease. Furthermore, bioassays

Figure 2. (continued).

ANMT; Rohde et al., 2008). Details of these other sequences are provided in Methods, and the full protein sequence alignment can be found in Supplemental Data Set 1 online. Bootstrap values (percentage of 1000 replicates) are shown for key branches. Bar indicates 0.05 substitutions per site.
(C) *Sad9* (*AsMT1*) transcript abundance in young leaves, whole roots, root tips (0.5 mm), and roots minus tips, measured by quantitative PCR (transcript abundance expressed relative to elongation factor 1-α); values are means ($n = 3 \pm$ SE).
(D) Immunostaining of root tip sections from 3-d-old wild-type *A. strigosa* seedlings. Sections were stained with (from left to right) anti-AsMT1 antisera, anti-AsSCPL1 antisera, or 4′,6-diamidino-2-phenylindole (DAPI). A bright-field image and an overlay of the MT1, SCPL1, and DAPI images are also shown. Controls probed with preimmune sera are shown in Supplemental Figure 1 online.

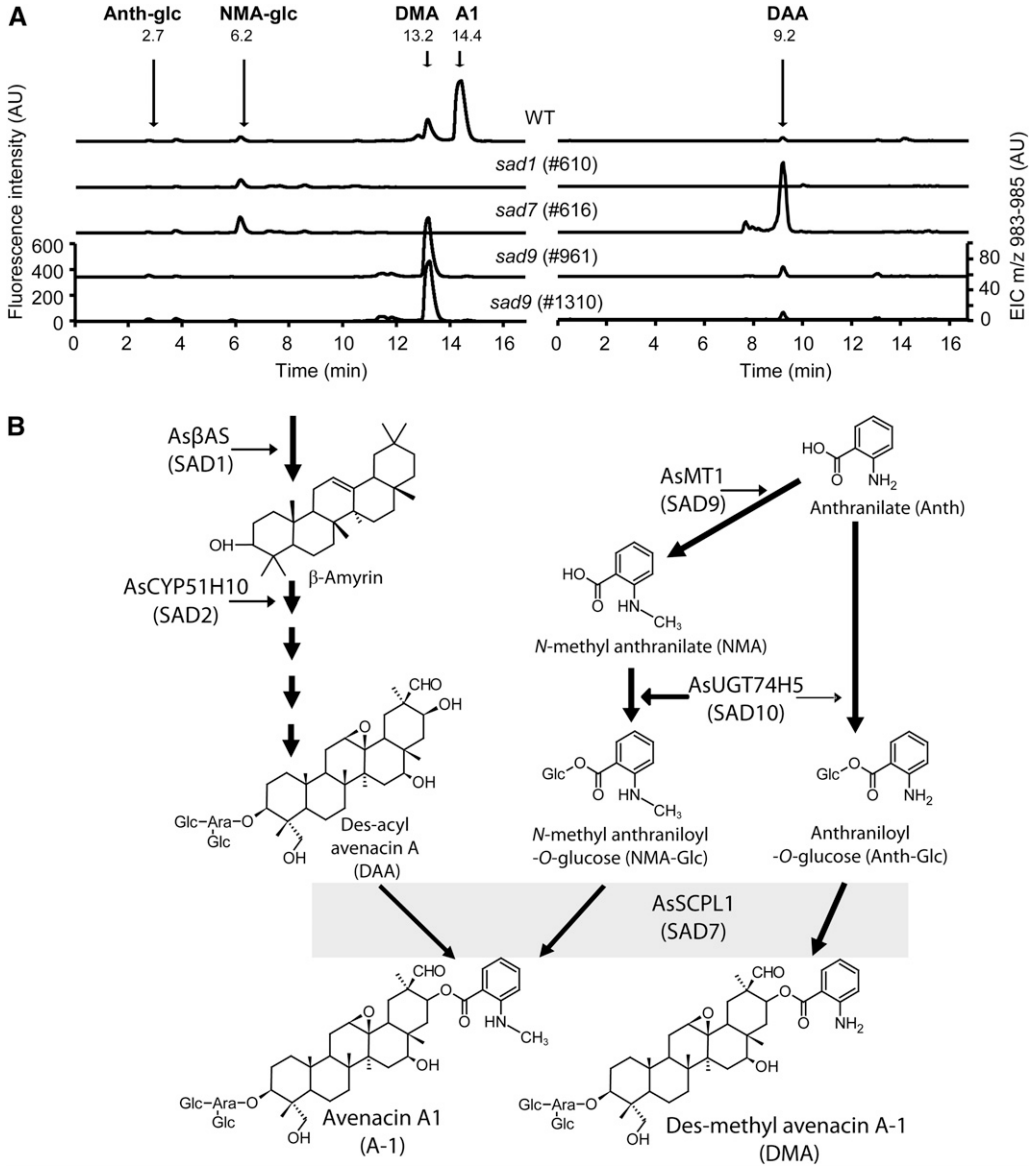

Figure 4. *sad9* Mutants Are Blocked in the Methylation of Avenacin Acyl-Groups.

(A) Analysis of wild-type and mutant (*sad1*, *sad7*, and *sad9*) root extracts by fluorescence LC-MS. Fluorescence detection shows the absence of avenacin A-1 (A1) in all mutants and the accumulation of DMA in *sad9* mutants. *N*-methyl anthraniloyl-*O*-Glc (NMA-glc) is not detectable in root extracts from *sad9* mutants, but anthraniloyl-*O*-Glc (Anth-glc) is detected at low levels. Similar metabolite profiles were observed in the other *sad9* mutants analyzed (see Supplemental Figure 2 online). Confirmation of the identity of these compounds by mass spectrometry is presented in Supplemental Figure 2 online. LC-MS shows the accumulation of des-acyl avenacin A (DAA; extracted ion chromatogram for mass-to-charge ratio = 983 to 985) in the *sad7* mutant, as previously shown by Mugford et al. (2009). AU, arbitrary units.

(B) Proposed pathway for acylation of avenacin A-1. *N*-methyl anthranilate (NMA) is synthesized by the methylation of anthranilate (Anth) by MT1. The glucosyltransferase UGT74H5 glucosylates *N*-methyl anthranilate to give the activated acyl donor substrate *N*-methyl anthraniloyl-*O*-Glc (NMA-Glc). UGT74H5 has a clear preference for *N*-methyl anthranilate but also has weak activity toward anthranilate to give anthraniloyl-*O*-Glc (Anth-Glc) (Owatworakit et al., 2012). In wild-type *A. strigosa*, the SCPL1 acyltransferase uses NMA-Glc as the acyl donor to give avenacin A-1 (A1). In *sad9* mutants (lacking MT1), the triterpenoid backbone is acylated with anthranilate instead of *N*-methyl anthranilate to give DMA.

with extracts from wild-type and *sad7* mutant root tips separated by thin layer chromatography (TLC) show that while avenacin A-1 in the wild-type sample strongly inhibits the growth of the indicator fungus *Colletotrichum orbiculare*, the presence of similar amounts of desacyl avenacin A in the *sad7* mutant extract has no such inhibitory effect (see Supplemental Figure 4 online). Thus, the acyl group is important for biological activity. The presence in the *sad9* mutants of benzoylated forms of avenacin in addition to DMA (see Supplemental Table 1 online) complicates efforts to establish the importance of the methyl

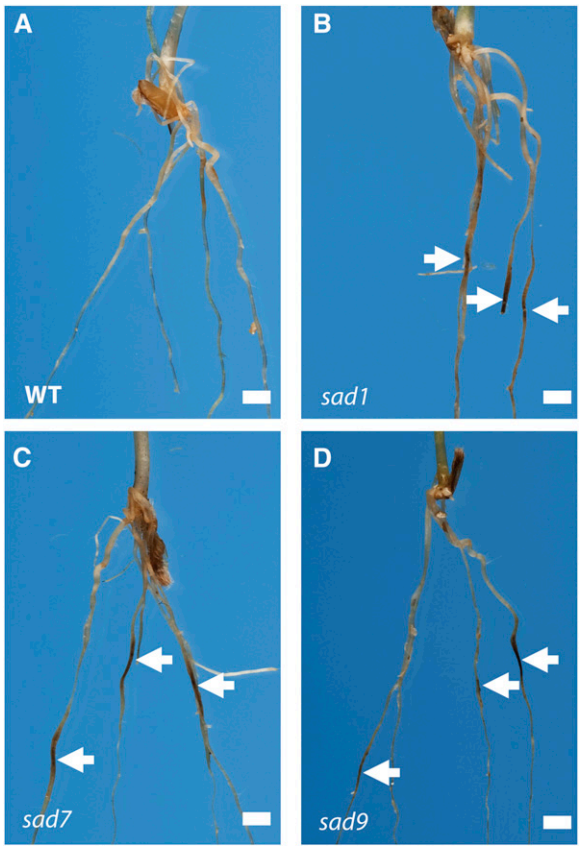

Figure 5. *sad9* Mutants Have Enhanced Disease Susceptibility.

Seedlings were inoculated with the take-all fungus (*G. graminis* var *tritici* strain T2) and scored for disease symptoms 3 weeks later as described by Papadopoulou et al. (1999). Dark-brown/black lesions on the roots (arrowed) are typical symptoms of infection. The wild type (WT) **(A)**, *sad1* mutant #610 **(B)**, *sad7* mutant #616 **(C)**, and *sad9* mutant #1475 **(D)**. Images are representative of six to 10 biological replicates across two independent experiments. Bars = 0.25 cm.

group for biological activity. However, a thin layer chromatography bioassay with extracts from *sad9* mutant roots clearly shows zones of *C. orbiculare* growth inhibition associated with both of the major forms of avenacin present in this mutant, desmethyl avenacin A-1 and avenacin A-2, indicating that desmethyl avenacin A-1 does possess antifungal activity (see Supplemental Figure 4 online). It is therefore likely that the increased susceptibility of *sad9* mutants to fungal infection is due to the overall lower concentrations of acylated avenacins relative to the wild type (see Supplemental Table 1 online).

MT1 was detected in protein preparations from the roots of wild-type *A. strigosa* seedlings and in *sad1* and *sad7* mutant lines. However, it was not detected in the four *sad9* mutants (Figure 3). The *sad9* mutants were isolated from a forward screen for loss-of-function mutations. Mutant #1310 has a premature stop codon, while, based on comparison with the structure of the *Medicago truncatula* isoflavone *O*-methyltransferase (the most similar sequence to As-MT1 for which a crystal structure is available; National Center for Biotechnology Information accession number 2QYO_A), the amino acid substitutions in the other three mutants are all likely to disrupt α-helices integral to the structure of the protein. All four *sad9* mutants had wild-type levels of the SCPL1 (SAD7) and UGT74H5 (SAD10) proteins. Interestingly, the levels of SCPL1 (SAD7) protein were substantially reduced in *sad1* mutants, which are blocked in the first committed step in avenacin biosynthesis (Qi et al., 2004) (shown for *sad1* mutant #610 in Figure 3). Examination of the levels of SCPL1 (SAD7) protein in a wider range of early pathway mutants (Qi et al., 2004, 2006; Qin et al., 2010) revealed that the SCPL1 protein level is reduced or abolished in all *sad1* and *sad2* mutants, while the levels of the MT1 and UGT74H5 proteins were not substantially altered in these mutants (see Supplemental Figure 5 online). The levels of the *Sad7* transcript were not significantly altered in any of the mutants (see Supplemental Figure 5 online), suggesting that SCPL1 may be posttranscriptionally regulated. A scenario consistent with these data is that the triterpene backbone is required for the accumulation of SCPL1 protein, since mutants that are unable to synthesize this backbone fail to accumulate SCPL1.

MT1 Encodes an Anthranilate *N*-Methyltransferase

MT1 was expressed in *Escherichia coli* with a C-terminal 6XHis epitope tag and purified by metal affinity chromatography. Accumulation of des-methyl avenacin and anthraniloyl-*O*-Glc in the *sad9* mutants indicates that the likely substrate for this enzyme in planta is either anthranilate or anthraniloyl-*O*-Glc. We found no detectable activity of the recombinant protein against anthraniloyl-*O*-Glc at a range of substrate concentrations (0.5 to 5 mM), while under the same conditions, MT1 effectively catalyzed the formation of *N*-methyl anthranilate from anthranilate. Kinetic analysis of the MT1 enzyme in vitro showed that the enzyme has a strong affinity for anthranilic acid (K_m = 5.51 ± 0.11 μM), with a pH optimum of 8.0, and a high catalytic efficiency (k_{cat}/K_m = 5.55 ± 0.16 nM^{-1} s^{-1}), which compare favorably with the reported kinetic properties of other plant methyl transferases that are active toward small phenolic compounds (Wang and Pichersky, 1999; Gang et al., 2002; Rohde et al., 2008; Jonczyk et al., 2008). Thus, As-MT1 catalyzes the first committed step in the synthesis of the *N*-methyl anthraniloyl acyl donor that is used by the As-SCPL1 acyltransferase, namely, methylation of the primary shikimate pathway intermediate anthranilate. This is consistent with the proposed pathway in Figure 4B and with the catalytic properties of As-UGT74H5, which has a strong affinity for *N*-methyl anthranilate compared with anthranilate (Owatworakit et al., 2012).

Coexpression of As-MT1 and As-UGT74H5 in *Nicotiana benthamiana* Leaves Results in the Accumulation of *N*-Methyl Anthraniloyl-*O*-Glc

The above evidence coupled with the previous characterization of As-SCPL and As-UGT74H5 (Mugford et al., 2009; Owatworakit et al., 2012) implicates As-MT1, As-UGT74H5, and As-SCPL1 in the synthesis and transfer of the *N*-methyl anthraniloyl acyl group onto the triterpene backbone. To further test the roles of these enzymes, we transiently coexpressed the As-*MT1*, As-*UGT74H5*, and As-*SCPL1* cDNAs in *N. benthamiana* leaves using a cowpea mosaic virus (CPMV)–derived expression system (Sainsbury et al.,

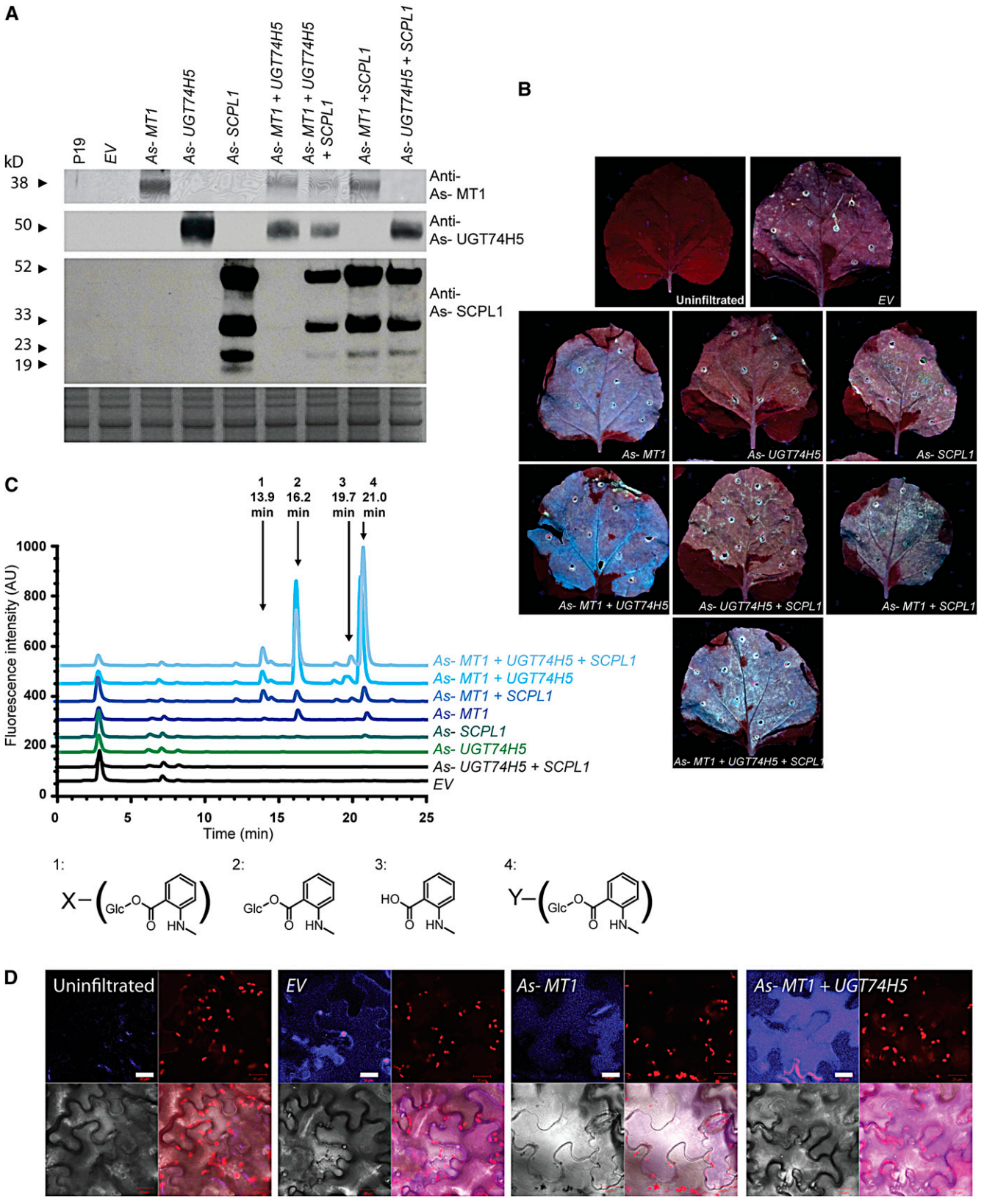

Figure 6. Coexpression of As-MT1 and As-UGT74H5 in Tobacco Leaves Results in the Accumulation and Sequestration of *N*-Methyl Anthraniloyl-*O*-Glc. **(A)** Immunoblot analysis of soluble protein extracts of *N. benthamiana* leaves probed with antisera raised against MT1, UGT74H5, and SCPL1. The bottom panel shows a replicate gel stained with Coomassie blue. Lanes were loaded with protein extracted from leaves 6 d after infiltration with-*Agrobacterium tumefaciens* strains containing (from left to right) the P19 silencing suppressor alone (P19) or in combination with the CPMV empty vector (*EV*); vectors containing the coding sequences of *MT1*, *UGT74H5*, or *SCPL1* alone or coinfiltrated in combination as indicated.

2008; Mugford et al., 2009) (Figure 6). Immunoblot analysis confirmed the expression of the three proteins, expressed either alone or in combination (Figure 6A). Interestingly, expression of MT1 alone was sufficient to cause the leaves to fluoresce blue under UV illumination, reminiscent of the fluorescence of oat root tips (Figure 6B), and this fluorescence was enhanced when MT1 and UGT74H5 were expressed in combination. HPLC analysis of methanolic extracts of the leaf material revealed that the expression of MT1 and UGT74H5 together results in the accumulation of *N*-methyl anthraniloyl-*O*-Glc (39.8 ± 6.5 nmol/mg fresh weight) (Figure 6C; see Supplemental Table 2 online). Expression of UGT74H5 alone did not lead to the production of detectable levels of any fluorescent compounds. Expression of the SCPL1 acyltransferase together with MT1 and UGT74H5 did not lead to accumulation of any additional detectable fluorescent compounds, indicating that SCPL1 is unlikely to be able to acylate endogenous compounds in *N. benthamiana*, which is perhaps not surprising since there are no reports of triterpenoid saponins or related compounds in this species. Further analysis by LC-MS failed to identify any other compounds that accumulated in an SCPL1-dependent manner. The expression of MT1 alone led to the accumulation of low levels of *N*-methyl anthranilate and *N*-methyl anthraniloyl-*O*-Glc, suggesting that *N. benthamiana* possesses enzymes capable of glucosylating *N*-methyl anthranilate at low levels, presumably as a side reaction of an endogenous glucosyltransferase. Also, two other fluorescent compounds were found to accumulate in leaves expressing MT1 and UGT74H5 together (and at lower levels in leaves expressing MT1 alone). These were identified by LC-MS as derivatives of *N*-methyl anthraniloyl-*O*-Glc, apparently modified by the addition of a hexose or malate residue, respectively (Figure 6C; see Supplemental Table 2 and Supplemental Figure 6 online) and are likely to have arisen as a result of endogenous *N. benthamiana* enzyme activities acting on *N*-methyl anthraniloyl-*O*-Glc. Confocal microscopy of *N. benthamiana* leaves suggests that the fluorescent material generated by coexpression of MT1 and UGT74H5 is located in the vacuole (Figure 6D).

Subcellular Localization of the Components of the Avenacin Acylation Pathway

Avenacins accumulate in the vacuoles of the epidermal cells of oat root tips (Mylona et al., 2008). However, the primary shikimate pathway leading to the synthesis of the precursors of the acyl groups is expected to be cytosolic or, more likely, plastidial (Radwanski and Last, 1995; Schmid and Amrhein, 1995). Immunogold labeling of epidermal cells in ultrathin sections of 3-d-old oat root tips was performed using antisera raised against SCPL1, UGT74H5, or MT1 (Figure 7; see Supplemental Table 3 online). The density of gold particles associated with different cellular compartments was determined across replicate samples probed with either specific antisera or the corresponding preimmune sera (see Supplemental Table 3 online). The MT1 antisera principally labeled the cytosol in wild-type oat root epidermal cells. Signal was not detected in the control *sad9* mutant line #961 or in samples probed with the corresponding preimmune sera (Figures 7A and 7B; see Supplemental Table 3 online). Sections taken from *N. benthamiana* leaves expressing MT1 protein were also probed with the anti-AsMT1 antisera (Figures 7C and 7D; see Supplemental Table 3 online). These were found to show strong labeling mainly in the cytosol, whereas empty vector control samples and samples probed with the preimmune sera did not give significant signals (see Supplemental Table 3 online).

Antisera raised against UGT74H5 labeled the cytoplasm and also the vacuole in wild-type oat root samples (Figure 7E) but not in samples probed with the corresponding preimmune sera (see Supplemental Table 3 online) (mutants lacking the UGT74H5 protein are not available). It should be noted that two close homologs of UGT74H5 are also expressed in oat roots and cross-react with the anti-AsUGT74H5 antisera (Owatworakit et al., 2012). To determine the localization of UGT74H5 in the absence of these other proteins, sections of *N. benthamiana* leaves expressing UGT74H5 were probed with the anti-AsUGT74H5 antisera. Strong labeling of the cytosol but not the vacuole was observed (Figures 7F and 7G; see Supplemental Table 3 online). This labeling was not seen in empty vector controls or in samples probed with the corresponding preimmune sera (see Supplemental Table 3 online). This suggests that UGT74H5 may also be restricted to the cytosol in oat roots and that the signal obtained from the vacuole in oat roots might be attributable to one of the close homologs of UGT74H5.

The SCPL1 antiserum specifically labeled the vacuole in wild-type oat roots. No labeling was seen in *sad7* mutants, which lack SCPL1, or in samples probed with preimmune serum (Figures 7H and 7I; see Supplemental Table 3 online). Taken together,

Figure 6. (continued).

(B) Leaves of *N. benthamiana* photographed under UV illumination 6 d after infiltration with *Agrobacterium* strains.

(C) HPLC analysis with fluorescence detection (excitation at 353 nm; emission at 441 nm) of methanolic extracts from *N. benthamiana* leaves. Peaks 2 and 3 are *N*-methyl anthraniloyl-*O*-Glc and *N*-methyl anthranilic acid, respectively. Peaks 1 and 4 were found to be derivatives of *N*-methyl anthraniloyl-*O*-Glc, which were further modified. Accurate mass determination and fragmentation by MS2 provides putative identification of the additional group on compound 1 (X) as a hexose and on compound 2 (Y) as malate (see Supplemental Figure 6 online). AU, arbitrary units.

(D) Confocal microscopy of lower epidermal cells of leaves (from left to right) uninfiltrated or infiltrated with *Agrobacterium* strains bearing the CPMV empty vector (EV), the CPMV vector carrying the *MT1* (*Sad9*) coding sequence, or *MT1* and *UGT74H5*. Clockwise from top left for each set of four panels: UV fluorescence, chlorophyll autofluorescence, overlay, and transmitted light. Blue fluorescence is detectable across the central body of cells coexpressing *MT1* and *UGT74H5* (and more weakly, also from cells expressing *MT1* alone), consistent with vacuolar compartmentalization of the fluorescent metabolites. The epidermal cells are highly vacuolated; the chlorophyll autofluorescence shows how the chloroplasts are restricted to the periphery of the cells by the enlarged vacuole. Conversely, weak blue fluorescence in the empty vector control leaves is mainly associated with the cell wall; this may be due to a response to *Agrobacterium* infiltration. Bars = 20 μm.

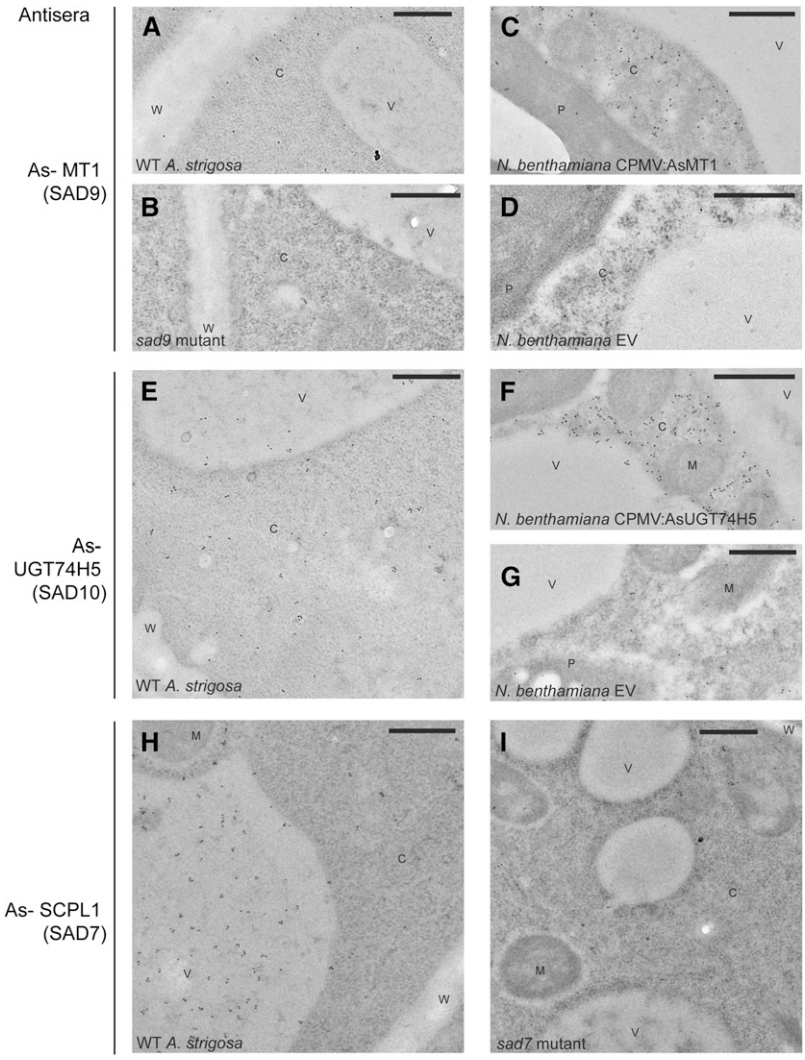

Figure 7. Subcellular Localization of As-MT1, As-UGT74H5, and As-SCPL1.

(A) to **(D)** Transmission electron microscopy images from immunogold labeling of ultrathin sections probed with antisera raised against MT1.
(A) and **(B)** Root tip epidermal cells of 3-d-old wild-type (WT) **(A)** and *sad9* (#961) mutant **(B)** oat seedlings.
(C) and **(D)** Sections from *N. benthamiana* leaves expressing the *CPMV-AsMT1* construct **(C)** or the *CPMV-EV* control **(D)**.
(E) to **(G)** Sections probed with antisera raised against UGT74H5.
(E) Wild-type oat root tip epidermis.
(F) and **(G)** *N. benthamiana* leaves expressing *CPMV-AsUGT74H5* **(F)** or *CPMV-EV* **(G)**.
(H) and **(I)** Sections probed with antisera raised against SCPL1. Wild-type **(H)** or *sad7* (#616) **(I)** mutant oat root tip epidermis.
Gold particle labeling is visible as black dots. Selected subcellular compartments are labeled as follows: C, cytoplasm; V, vacuole; P, plastid; M, mitochondria; and W, cell wall. Images are representative of 10 to 20 biological replicates, and quantification of gold particle densities in different compartments is presented in Supplemental Table 2 online. Bars = 0.5 μm.

our localization experiments suggest a model for the organization of the pathway as shown in Figure 8.

DISCUSSION

We have shown that three consecutive genes within the avenacin gene cluster are involved in the acylation of avenacins at the C-21 position and that the failure to correctly acylate avenacins results in enhanced disease susceptibility. This is in line with the finding that C-21 acylation is a common feature of many of the most cytotoxic triterpenoid glycosides, suggesting that it is a key contributor to the biological activity of these compounds (Podolak et al., 2010). The identification of a cassette of genes for triterpene acylation is thus of practical significance and opens up opportunities for triterpene modification using metabolic engineering approaches.

The biochemical characterization and localization data presented here suggest a model for the subcellular organization of the

triterpene pathway as shown in Figure 8. The shikimate pathway intermediate anthranilate is methylated and subsequently glucosylated in the cytosol, producing the activated acyl donor *N*-methyl anthraniloyl-*O*-glucose. This compound is then transported into the vacuole where it serves as a substrate for SCPL1. Evidence for the transport of *N*-methyl anthraniloyl-*O*-Glc comes from *sad7* mutants, which accumulate this compound, where it can be seen that the fluorescence originates from the vacuole (see Supplemental Figure 7 online). The capacity to transport the acyl donor substrate into the vacuole is also present in *N. benthamiana* (Figure 6D). The identity of the transporter(s) involved remains to be established. Previous reports of the localization of members of the *S*-adenosyl Met-dependent methyltransferase and family 1 glucosyltransferase families indicate that most of these enzymes are in the cytosol (Yazaki et al., 1995; Ruelland et al., 2003; Achnine et al., 2005; Dhaubhadel et al., 2008; Hugueney et al., 2009), although members of both families have been reported in other compartments (Halkier and Møller, 1989; Anhalt and Weissenböck, 1992; Ibrahim, 1992; Jones and Vogt, 2001). The localization of the As-SCPL1 acyltransferase to the vacuole is consistent with predictions for this family (Fraser et al., 2005; Mugford et al., 2009) and with experimental data for one other SCPL acyltransferase, which was found to be vacuolar (Hause et al., 2002).

An interesting aspect of the regulation of the avenacin biosynthetic pathway has emerged as a part of this work. We found

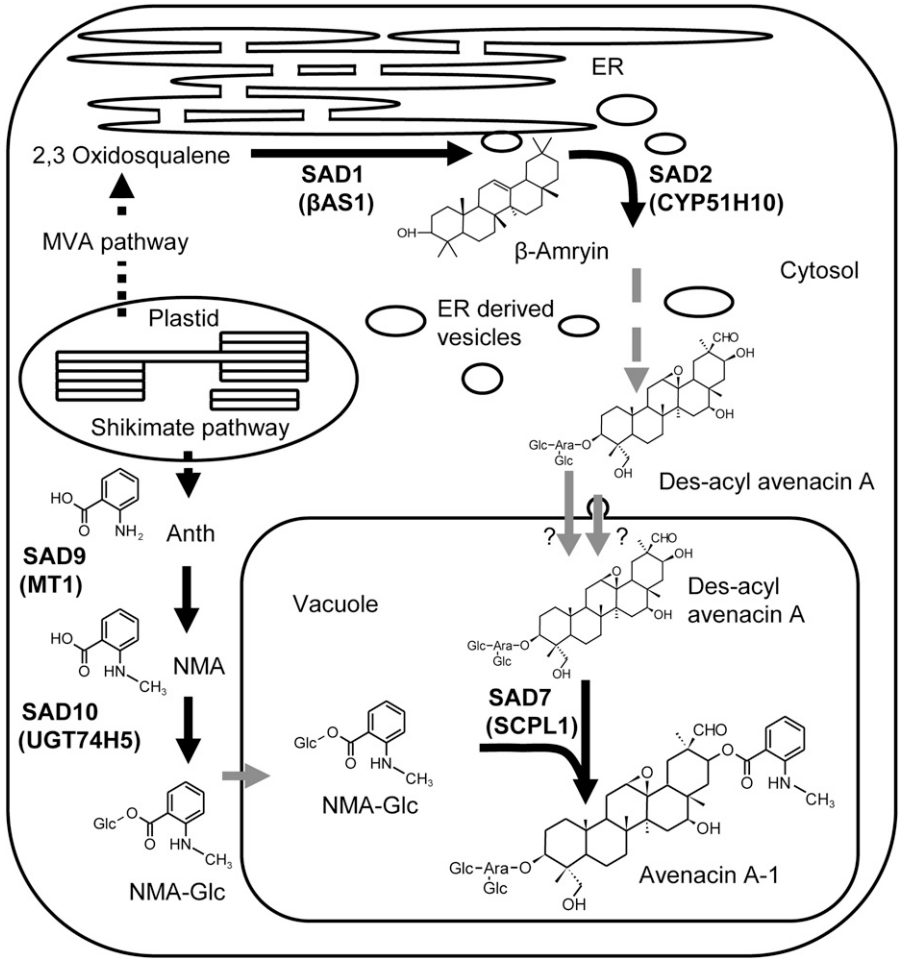

Figure 8. Model of the Subcellular Organization of Avenacin A-1 Biosynthesis in Oat.

The acyl group of avenacin A-1 originates from the shikimate pathway in the plastid. Anthranilate (Anth) (which fluoresces purple under UV illumination) is methylated by MT1 (encoded by *Sad9*) to produce *N*-methyl anthranilate (NMA) (which fluoresces blue) and then glucosylated by *UGT74H5* to give *N*-methyl anthraniloyl-*O*-glucose (NMA-Glc). NMA-Glc is transported into the vacuole by an unknown mechanism, where it serves as the acyl donor substrate for SCPL1 (SAD7). The triterpene glycoside is synthesized from the cytoplasmic mevalonate (MVA) pathway products, and the early steps are catalyzed by β-amyrin synthase (SAD1/AsβAS1) and CYP51H10 (SAD2). These steps are likely to be associated with the endoplasmic reticulum (ER) membrane (Wegel et al., 2009). Des-acyl avenacin A is then formed by a series of as yet uncharacterized oxidation and glycosylation steps. The triterpene glycoside is transported into the vacuole, either by a vacuolar membrane transporter or possibly through vesicular trafficking from the endoplasmic reticulum to the vacuole.

that the As-SCPL1 acyltransferase protein, which catalyzes the final step in avenacin biosynthesis, was not detectable in mutants that are blocked in early stages of the pathway (*sad1* and *sad2* mutants) but was detectable in mutants blocked late in the pathway (*sad7* and *sad9* mutants; Figure 3; see Supplemental Figure 2 online). As-*SCPL1* transcript levels were not altered in any of the mutants tested (see Supplemental Figure 2 online). This suggests that the levels of As-SCPL1 may be subject to post-transcriptional regulation, possibly in response to the presence of an intermediate in the avenacin biosynthetic pathway. This regulatory mechanism seems to be specific to As-SCPL1, since other avenacin biosynthetic enzymes are not affected in the same way. This adds another level of regulation to the tight cotranscriptional regulation that restricts the expression of the avenacin gene cluster to root tip epidermal cells.

The mechanisms by which plant natural product gene clusters form are not understood. It has been speculated that the formation of gene clusters encoding plant natural product biosynthetic pathways is associated with the toxicity of pathway intermediates and is driven by selection to prevent partial pathway inheritance (Takos and Rook, 2012). However, we found that the *sad9* mutants do not exhibit any obvious growth defects or other abnormalities that might be expected as a result of the accumulation of a toxic intermediate compound. This is similar in the case of other mutants blocked in this pathway, with the exception of the *sad3* and *sad4* mutants, which accumulate a toxic form of avenacin that is incompletely glucosylated and that disrupts root development (Mylona et al., 2008). While containment of toxic intermediates may contribute to the selection driving the evolution of plant natural product gene clusters, it seems likely that other factors, such as coinheritance of beneficial combinations of alleles of the different pathway genes and coordinated regulation at the level of chromatin, are also likely to be important (Wegel et al., 2009; Chu et al., 2011).

Previously, we reported that several of the avenacin biosynthetic genes bear signatures of recent and strong selective pressure (Qi et al., 2004, 2006; Mugford et al., 2009; Mugford and Osbourn, 2010), consistent with a change of function since the divergence of these sequences from their relatives in other species. It remains to be established whether the neofunctionalization of these enzymes preceded the clustering of their genes or vice versa. In-depth phylogenetic analysis coupled with comparative genomics for all of these large multigene families will be required to address these questions.

METHODS

Plant Material

The wild-type and mutant *Avena strigosa* lines used in this study are described by Papadopoulou et al. (1999), Qi et al. (2006), and Mugford et al. (2009). Pathogenicity assays were performed as previously described (Papadopoulou et al., 1999).

BAC Contig Expansion and Expression Analysis

The *A. strigosa* BAC contig spanning the *Sad1*, *Sad2*, *Sad7*, and *UGT74H5* (*Sad10*) genes has been previously described (Qi et al., 2006; Mugford et al., 2009; Owatworakit et al., 2012). Overlapping BAC clones were identified by screening the BAC library with single/low-copy number probes from the ends of BAC clones and verified by PCR and restriction mapping. New BAC clones were verified by shotgun sequencing.

The predicted full-length coding sequence of the *Sad9* gene was amplified by PCR and cloned into the pET24a vector (Novagen) with the addition of sequence encoding a 6XHis epitope tag to the C terminus of the protein. The His-tagged Sad9 protein was expressed in *Escherichia coli* (BL21) and purified by Ni-affinity chromatography and subsequently by gel filtration chromatography according to standard methods. Purified protein (1 mg) was supplied to Biogenes for the production of antisera in rats. Immunoblot analysis was performed as described by Mugford et al., (2009), and the anti-Sad9 antisera was used at a dilution of 1:500.

RNA was extracted and cDNA synthesized as described previously (Qi et al., 2006).

Quantitative real-time PCR was performed using a Bio-Rad CFX96 real-time system C1000 thermal cycler using SYBR Green JumpStart Taq ReadyMix for quantitative PCR (Sigma-Aldrich). Oligonucleotide sequences used were *Ef1*α, 5′-TCCCCATCTCTGGATTTGAG-3′ and 5′-TCTCTTGGGCTCGTTGATCT-3′; As-*SCPL1*, 5′-GCTTCACCGTCGAGTATTCC-3′ and 5′-GATCCATCTTCGGACCATGT-3′; and As-*MT1*, 5′-ACCCCACGACAACATCAAG-3′ and 5′-CGCGGTTCTACTCAAGTGGT-3′.

Phylogenetic Methods

Protein sequence alignment was performed using Muscle 3.6 (Edgar 2004), and the neighbor joining phylogeny was constructed using Mega 4.0 (Tamura et al., 2007). The full sequence alignment used to reconstruct the phylogeny can be found in Supplemental Data Set 1 online. Accession numbers for sequences included in the phylogeny are listed below. The abbreviations used are as follows: CNMT, (*S*)-coclaurine *N*-methyltransferase; 4OMT, (*S*)-3-hydroxy-*N*-methylcoclaurine 4-*O*-methyltransferase; 6OMT, (*S*)-norcoclaurine 6-*O*-methyltransferase; 7OMT, (*R*,*S*)-reticuline 7-*O*-methyltransferase; BANMT, β-Ala *N*-methyltransferase; BOMT, benzoic acid carboxyl methyltransferase; CaOMT, catechol *O*-methyltransferase; ChOMT, chavicol *O*-methyltransferase; COMT, caffeic acid *O*-methyltransferase; CoOMT, columbamine *O*-methyltransferase; DMXNMT, dimethylxanthine *N*-methyltransferase; EOMT, (iso)eugenol *O*-methyltransferase; FOMT, flavonoid 8-*O*-methyltransferase; MXNMT, 7-methylxanthine *N*-methyltransferase; PEANMT, phosphoethanolamine *N*-methyltransferase; PNMT, putrescine *N*-methyltransferase; SAMT, salicylic acid carboxyl methyltransferase; SOMT, scoulerine 9-*O*-methyltransferase; and XNMT, xanthosine methyltransferase.

sad9 Mutant Identification and Metabolite Analysis

Previously uncharacterized avenacin-deficient *A. strigosa* mutants (Papadopoulou et al., 1999; Qi et al., 2006) were screened for single nucleotide polymorphisms in the *Sad9* gene using the Surveyor mutation detection kit (Transgenomic) according to the manufacturer's protocol and candidates verified by sequencing. Metabolites were extracted from root tips of 5-d-old seedlings as described previously (Mugford et al., 2009). Fluorescent compounds were analyzed by LC-MS, coupled with fluorescence detection (Mugford et al., 2009). Glc esters of anthranilate and *N*-methyl anthranilate were quantified by HPLC (also described in Mugford et al., 2009).

Biochemical Characterization of As-MT1

Activity assays were performed using 4 μg of purified recombinant As-MT1 protein in 50 mM Tris-HCl, pH 8.0, and 2.5 mM *S*-adenosyl-Met, in a volume of 200 μL at 30°C. Reactions were started by the addition of the methyl acceptor substrate and stopped after 7 min by the addition of 10 μL of trichloro-acetic acid (TCA). For the determination of kinetic parameters, activity was tested at anthranilate concentrations ranging from 0.05 to 7.5 mM and anthraniloyl-*O*-Glc from 0.5 to 5 mM, each tested in triplicate.

Concentrations of methylated product were determined by HPLC using a Dionex UltiMate 3000 HPLC with a Luna C18 160 × 4, 60-mm column (Phenomenex) running a gradient of acetonitrile against 0.1% trifluoroacetic acid in water from 10 to 90% over 22 min. The flow rate was constant at 0.5 mL/min, the injection volume was 60 μL, and the detection wavelength used was 320 nm. Data were plotted as a Lineweaver-Burk plot, and Michaelis-Menten kinetic parameters were determined.

CPMV-Based Coexpression

The coding sequences of the As-*MT1*, As-*SCPL1*, and As-*UGT74H5* cDNAs were amplified by PCR and cloned into the modified *pM81S2NT* plasmid (Cañizares et al., 2006) to flank the sequences by the 5′ and 3′ untranslated regions of CPMV *RNA-2* prior to transfer to pBINPLUS. Expression from the cassette was under control of the cauliflower mosaic virus 35S promoter. Constructs were transformed into *Agrobacterium tumefaciens* LBA4404 and infiltrated into *Nicotiana benthamiana* leaves as described previously (Cañizares et al., 2006; Mugford et al., 2009). For coexpression experiments, *Agrobacterium* cultures carrying each of the three constructs were mixed prior to infiltration or were diluted in infiltration medium for expression alone. Leaves were harvested after 6 d and snap-frozen in liquid nitrogen or photographed under UV illumination. Metabolite extracts and immunoblot analysis was performed as described previously (Mugford et al., 2009). Accurate mass identification of unknown metabolites was performed by LC-MS. Compounds were separated on a 50 × 2-mm 3-μ Luna C18(2) column (Phenomenex) on a Surveyor HPLC system (Thermo Finnigan) using a gradient of methanol versus 0.1% formic acid in water from 10 to 80% over 20 min. The column outflow was connected directly to an Orbitrap mass spectrometer electrospray spray chamber (Thermo Finnigan) using spray chamber conditions of 250°C capillary temperature, 32 units sheath gas, 6 units aux gas, 4.3-kV spray voltage, and tube lens voltage of 40 V. The Orbitrap was set up to collect full mass spectra at a resolution of 60,000 from mass-to-charge ratio 160 to 1500 and to collect data dependent MS2 at a resolution of 15,000. MS2 was collected by Fourier Transform Mass Spectrometry (FTMS). MS2 was performed by collision-induced dissociation at 35% collision energy and with an isolation width of 2.0.

Confocal microscopy was performed on leaf sections from infiltrated plants and on whole oat roots using a Zeiss LSM510 microscope, with illumination from a violet diode laser at 405 nm.

Immunostaining

For immunofluorescence staining, roots were harvested from 5-d-old seedlings, fixed in 2% formaldehyde, and sectioned on a vibratome (50 μm). Sections were digested for 1 h with 1% driselase, 0.5% cellulose, and 0.025% pectolyase (Duchefa), preincubated in 3% BSA in tris-buffered saline (TBS) for 30 min, and then incubated for 1 h with the antisera (or preimmune sera). Anti-AsMT1 antisera was used at 1:200 dilution and anti-AsSCPL1 antisera at 1:1000 dilution. Incubations were performed overnight at 4°C, followed by washing in TBS. Sections were then incubated in a 1:200 dilution of fluorescent dye–conjugated secondary antibodies (Life Technologies; goat anti-rabbit-alexa488 for As-SCPL1 and goat anti-rat-alexa456 for As-MT1) in 3% BSA in TBS for 1 h, washed in TBS, stained in 1 μg/mL 4′,6-diamidino-2-phenylindole for 5 min, and imaged using a Nikon Eclipse e600 microscope.

Tissue fixation for immunogold labeling was performed as by Simpson et al. (2009).

Primary antibodies were used at the following dilutions: 1/100 for anti-AsMT1; 1/200 for anti-AsUGT74H5 and 1/500 for anti-AsSCPL1, with 1/50 goat anti-rabbit (for As-UGT74H5 and As-SCPL1) or goat anti-rat (for As-MT1) secondary antibody conjugated to 10-nm gold particles (BioCell, Agar Scientific). The grids were viewed in a Tecnai 20 transmission electron microscope (FEI) at 200 kV, and digital TIFF images were taken using an AMT XR60B digital camera (Deben).

Accession Numbers

The sequence of the *Sad9* gene can be found in GenBank under accession number JQ071450. Sequences included in the phylogenetic tree in Figure 2 are as follows: *Thalictrum flavum* 6OMT, AAU20765; *Coptis japonica* 6OMT, BAB08004; *Papaver somniferum* 6OMT, AAQ01669; *P. somniferum* 4OMT, AAP45313; *T. flavum* 4OMT, AAU20768; *C. japonica* 4OMT, BAB08005; *C. japonica* CoOMT, BAC22084; *A. strigosa* MT1, JQ071450; *Mentha x piperita* FOMT, AY337459; *Ocimum basilicum* EOMT, AAL30424; *O. basilicum* ChOMT, AAL30423; *P. somniferum* 7OMT, AAQ01668; *Limonium latifolium* BANMT, AAP03058; *T. flavum* SOMT, AAU20770; *C. japonica* SOMT, BAA06192; *Ammi majus* COMT, AAR24095; *R. graveolens* ANMT, DQ884932; *P. somniferum* CaOMT, AAQ01670; *O. basilicum* COMT1, AAD38189; *O. basilicum* COMT2, AF154918; *Clarkia breweri* EOMT, AAC01533; *C. breweri* COMT, O23760; *Atropa belladonna* PNMT, BAA82264; *Datura stramonium* PNMT, CAE47481; *Solanum lycopersicum* PEANMT, AAG59894; *Coffea arabica* DMXNMT1, BAC75663; *C. arabica* MXNMT, BAB39216; *C. arabica* XNMT, BAB39215; *Camellia sinensis* DMXNMT, BAB12278; *Antirrhinum majus* BOMT, AAF98284; *C. breweri* SAMT, AAF00108; *Mesorhizobium loti* CFAPS, BAB53730; *Arabidopsis* At4g33110, AAM65762; *Arabidopsis* At4g33120, ORF NP 195038; *P. somniferum* CNMT, AAP45316; *T. flavum* CNMT, AAU20766; and *C. japonica* CNMT, BAB71802.

Supplemental Data

The following materials are available in the online version of this article.

Supplemental Figure 1. Wild-Type Oat Root Sections Probed with Preimmune Sera.

Supplemental Figure 2. Identification of Des-Methyl Avenacin A-1 and Anthraniloyl-*O*-Glc by LC-MS.

Supplemental Figure 3. ^{1}H-NMR Spectra of the Avenacin C30-Aldehyde Region in Oat Root Extracts.

Supplemental Figure 4. Acylation of Avenacins Is Important for Biological Activity.

Supplemental Figure 5. As-SCPL1 Expression Is Reduced or Abolished in Oat Mutants Blocked in the Early Steps in the Synthesis of the Avenacin Triterpene.

Supplemental Figure 6. LC-MS Analysis of Fluorescent Compounds from *N. benthamiana* Plants Coexpressing As-MT1 and As-UGT74H5.

Supplemental Figure 7. Fluorescent Compounds Accumulate in the Vacuole of *sad7* Mutants.

Supplemental Table 1. Quantification of Avenacins and Des-Methyl Avenacin A-1 in Wild-Type and Mutant Oat Root Tips.

Supplemental Table 2. Quantification of Fluorescent Compounds in *N. benthamiana* Leaves Coexpressing Avenacin Biosynthetic Enzymes.

Supplemental Table 3. Subcellular Localization of the As-MT1, As-UGT74H5, and As-SCPL1 Proteins.

Supplemental Data Set 1. Protein Sequence Alignment Used in Phylogenetic Analysis.

ACKNOWLEDGMENTS

We thank Kim Findlay and Sue Bunnewell for immunogold labeling and transmission electron microscopy, Grant Calder for confocal microscopy, and Ian Colquhoun for NMR. This project was funded by the Biotechnology and Biological Sciences Research Council, UK (Grant BB/

E009912/1 to S.T.M.), by a joint Engineering and Physical Sciences Research Council/National Science Foundation award to A.O. and S.J.R. as part of the Syntegron Consortium (EP/H019154/1), and by the University of Glasgow work placement program (S.H.). R.M., L.H., G.P.L., and A.O. are supported by the Biotechnology and Biological Sciences Research Council Institute Strategic Program Grant "Understanding and Exploiting Plant and Microbial Secondary Metabolism" (BB/J004561/1) and the John Innes Foundation.

AUTHOR CONTRIBUTIONS

S.T.M, T.L., R.M., X.Q., S.B., T.T., L.H., and S.H. performed the research. S.T.M., X.Q., G.P.L, S.J.R., and A.O. designed the research. S.T.M. and A.O. wrote the article.

Received February 7, 2013; revised February 25, 2013; accepted March 5, 2013; published March 29, 2013.

REFERENCES

Achnine, L., Huhman, D.V., Farag, M.A., Sumner, L.W., Blount, J.W., and Dixon, R.A. (2005). Genomics-based selection and functional characterization of triterpene glycosyltransferases from the model legume *Medicago truncatula*. Plant J. **41:** 875–887.

Anhalt, S., and Weissenböck, G. (1992). Subcellular localization of luteolin glucuronides and related enzymes in rye mesophyll. Planta **187:** 83–88.

Baumert, A., Milkowski, C., Schmidt, J., Nimtz, M., Wray, V., and Strack, D. (2005). Formation of a complex pattern of sinapate esters in *Brassica napus* seeds, catalysed by enzymes of a serine carboxypeptidase-like acyltransferase family. Phytochemistry **66:** 1334–1345.

Cañizares, M.C., Liu, L., Perrin, Y., Tsakiris, E., and Lomonossoff, G.P. (2006). A bipartite system for the constitutive and inducible expression of high levels of foreign proteins in plants. Plant Biotechnol. J. **4:** 183–193.

Chu, H.Y., Wegel, E., and Osbourn, A. (2011). From hormones to secondary metabolism: The emergence of metabolic gene clusters in plants. Plant J. **66:** 66–79.

Crombie, L., Crombie, W.M.L., and Whiting, D.A. (1984). Structure of the four avenacins, oat root resistance factors to take-all disease. J. Chem. Soc. Chem. Commun. **4:** 246–248.

D'Auria, J.C. (2006). Acyltransferases in plants: A good time to be BAHD. Curr. Opin. Plant Biol. **9:** 331–340.

Dhaubhadel, S., Farhangkhoee, M., and Chapman, R. (2008). Identification and characterization of isoflavonoid specific glycosyltransferase and malonyltransferase from soybean seeds. J. Exp. Bot. **59:** 981–994.

Dixon, R.A. (2001). Natural products and plant disease resistance. Nature **411:** 843–847.

Dudareva, N., D'Auria, J.C., Nam, K.H., Raguso, R.A., and Pichersky, E. (1998). Acetyl-CoA:benzylalcohol acetyltransferase—An enzyme involved in floral scent production in *Clarkia breweri*. Plant J. **14:** 297–304.

Edgar, R.C. (2004). MUSCLE: Multiple sequence alignment with high accuracy and high throughput. Nucleic Acids Res. **32:** 1792–1797.

Falara, V., Akhtar, T.A., Nguyen, T.T., Spyropoulou, E.A., Bleeker, P.M., Schauvinhold, I., Matsuba, Y., Bonini, M.E., Schilmiller, A.L., Last, R.L., Schuurink, R.C., and Pichersky, E. (2011). The tomato terpene synthase gene family. Plant Physiol. **157:** 770–789.

Field, B., Fiston-Lavier, A.-S., Kemen, A., Geisler, K., Quesneville, H., and Osbourn, A.E. (2011). Formation of plant metabolic gene clusters within dynamic chromosomal regions. Proc. Natl. Acad. Sci. USA **108:** 16116–16121.

Field, B., and Osbourn, A.E. (2008). Metabolic diversification—Independent assembly of operon-like gene clusters in different plants. Science **320:** 543–547.

Fraser, C.M., Rider, L.W., and Chapple, C. (2005). An expression and bioinformatics analysis of the *Arabidopsis* serine carboxypeptidase-like gene family. Plant Physiol. **138:** 1136–1148.

Fraser, C.M., Thompson, M.G., Shirley, A.M., Ralph, J., Schoenherr, J.A., Sinlapadech, T., Hall, M.C., and Chapple, C. (2007). Related *Arabidopsis* serine carboxypeptidase-like sinapoylglucose acyltransferases display distinct but overlapping substrate specificities. Plant Physiol. **144:** 1986–1999.

Frey, M., Chomet, P., Glawischnig, E., Stettner, C., Grün, S., Winklmair, A., Eisenreich, W., Bacher, A., Meeley, R.B., Briggs, S.P., Simcox, K., and Gierl, A. (1997). Analysis of a chemical plant defense mechanism in grasses. Science **277:** 696–699.

Fujiwara, H., Tanaka, Y., Yonekura-Sakakibara, K., Fukuchi-Mizutani, M., Nakao, M., Fukui, Y., Yamaguchi, M., Ashikari, T., and Kusumi, T. (1998). cDNA cloning, gene expression and subcellular localization of anthocyanin 5-aromatic acyltransferase from *Gentiana triflora*. Plant J. **16:** 421–431.

Gang, D.R., Lavid, N., Zubieta, C., Chen, F., Beuerle, T., Lewinsohn, E., Noel, J.P., and Pichersky, E. (2002). Characterization of phenylpropene O-methyltransferases from sweet basil: Facile change of substrate specificity and convergent evolution within a plant O-methyltransferase family. Plant Cell **14:** 505–519.

Gierl, A., and Frey, M. (2001). Evolution of benzoxazinone biosynthesis and indole production in maize. Planta **213:** 493–498.

Grienenberger, E., Besseau, S., Geoffroy, P., Debayle, D., Heintz, D., Lapierre, C., Pollet, B., Heitz, T., and Legrand, M.A.F. (2009). A BAHD acyltransferase is expressed in the tapetum of *Arabidopsis* anthers and is involved in the synthesis of hydroxycinnamoyl spermidines. Plant J. **58:** 246–259.

Halkier, B.A., and Møller, B.L. (1989). Biosynthesis of the cyanogenic glucoside dhurrin in seedlings of *Sorghum bicolor* (L.) Moench and partial purification of the enzyme system involved. Plant Physiol. **90:** 1552–1559.

Haralampidis, K., Bryan, G., Qi, X., Papadopoulou, K., Bakht, S., Melton, R., and Osbourn, A. (2001). A new class of oxidosqualene cyclases directs synthesis of antimicrobial phytoprotectants in monocots. Proc. Natl. Acad. Sci. USA **98:** 13431–13436.

Hause, B., Meyer, K., Viitanen, P.V., Chapple, C., and Strack, D. (2002). Immunolocalization of 1-*O*-sinapoylglucose:malate sinapoyltransferase in *Arabidopsis thaliana*. Planta **215:** 26–32.

Hostettmann, K., and Marston, A. (1995). Saponins: Chemistry and Pharmacology of Natural Products. (Cambridge, UK: Cambridge University Press).

Hugueney, P., Provenzano, S., Verriès, C., Ferrandino, A., Meudec, E., Batelli, G., Merdinoglu, D., Cheynier, V., Schubert, A., and Ageorges, A. (2009). A novel cation-dependent *O*-methyltransferase involved in anthocyanin methylation in grapevine. Plant Physiol. **150:** 2057–2070.

Ibrahim, R.K. (1992). Immunolocalization of flavonoid conjugates and their enzymes. In Phenolic Metabolism in Plants, H.A. Stafford and R.K. Ibrahim, eds (New York: Plenum Press), pp. 25–61.

Jonczyk, R., Schmidt, H., Osterrieder, A., Fiesselmann, A., Schullehner, K., Haslbeck, M., Sicker, D., Hofmann, D., Yalpani, N., Simmons, C., Frey, M., and Gierl, A. (2008). Elucidation of the final reactions of DIMBOA-glucoside biosynthesis in maize: characterization of Bx6 and Bx7. Plant Physiol. **146:** 1053–1063.

Jones, P., and Vogt, T. (2001). Glycosyltransferases in secondary plant metabolism: Tranquilizers and stimulant controllers. Planta **213:** 164–174.

Kliebenstein, D.J., and Osbourn, A. (2012). Making new molecules - Evolution of pathways for novel metabolites in plants. Curr. Opin. Plant Biol. **15:** 415–423.

Lehfeldt, C., Shirley, A.M., Meyer, K., Ruegger, M.O., Cusumano, J.C., Viitanen, P.V., Strack, D., and Chapple, C. (2000). Cloning of the *SNG1* gene of *Arabidopsis* reveals a role for a serine carboxypeptidase-like protein as an acyltransferase in secondary metabolism. Plant Cell **12:** 1295–1306.

Li, A.X., and Steffens, J.C. (2000). An acyltransferase catalyzing the formation of diacylglucose is a serine carboxypeptidase-like protein. Proc. Natl. Acad. Sci. USA **97:** 6902–6907.

Lim, E.K., Li, Y., Parr, A., Jackson, R., Ashford, D.A., and Bowles, D.J. (2001). Identification of glucosyltransferase genes involved in sinapate metabolism and lignin synthesis in *Arabidopsis*. J. Biol. Chem. **276:** 4344–4349.

Liscombe, D.K., and Facchini, P.J. (2007). Molecular cloning and characterization of tetrahydroprotoberberine cis-*N*-methyltransferase, an enzyme involved in alkaloid biosynthesis in opium poppy. J. Biol. Chem. **282:** 14741–14751.

Luo, J., Fuell, C., Parr, A., Hill, L., Bailey, P., Elliott, K., Fairhurst, S. A., Martin, C., and Michael, A.J. (2009). A novel polyamine acyltransferase responsible for the accumulation of spermidine conjugates in *Arabidopsis* seed. Plant Cell **21:** 318–333.

Luo, J., et al. (2007). Convergent evolution in the BAHD family of acyl transferases: Identification and characterization of anthocyanin acyl transferases from *Arabidopsis thaliana*. Plant J. **50:** 678–695.

Milkowski, C., Baumert, A., Schmidt, D., Nehlin, L., and Strack, D. (2004). Molecular regulation of sinapate ester metabolism in *Brassica napus*: Expression of genes, properties of the encoded proteins and correlation of enzyme activities with metabolite accumulation. Plant J. **38:** 80–92.

Milkowski, C., and Strack, D. (2004). Serine carboxypeptidase-like acyltransferases. Phytochemistry **65:** 517–524.

Mugford, S.T., and Milkowski, C. (2012). Serine carboxypeptidase-like acyltransferases from plants. Methods Enzymol. **516:** 279–297.

Mugford, S.T., and Osbourn, A. (2010). Evolution of serine carboxypeptidase-like acyltransferases in the monocots. Plant Signal. Behav. **5:** 193–195.

Mugford, S.T., et al. (2009). A serine carboxypeptidase-like acyltransferase is required for synthesis of antimicrobial compounds and disease resistance in oats. Plant Cell **21:** 2473–2484.

Mylona, P., Owatworakit, A., Papadopoulou, K., Jenner, H., Qin, B., Findlay, K., Hill, L., Qi, X., Bakht, S., Melton, R., and Osbourn, A. (2008). *Sad3* and *sad4* are required for saponin biosynthesis and root development in oat. Plant Cell **20:** 201–212.

Osbourn, A., Goss, R.J.M., and Field, R.A. (2011). The saponins: Polar isoprenoids with important and diverse biological activities. Nat. Prod. Rep. **28:** 1261–1268.

Osbourn, A.E., and Lanzotti, V. (2009). Plant-Derived Natural Products. (New York: Springer).

Owatworakit, A., et al. (2012). Glycosyltransferases from oat (*Avena*) implicated in the acylation of avenacins. J. Biol. Chem. **288:** 3696–3704.

Papadopoulou, K., Melton, R.E., Leggett, M., Daniels, M.J., and Osbourn, A.E. (1999). Compromised disease resistance in saponin-deficient plants. Proc. Natl. Acad. Sci. USA **96:** 12923–12928.

Podolak, I., Galanty, A., and Sobolewska, D. (2010). Saponins as cytotoxic agents: A review. Phytochem. Rev. **9:** 425–474.

Qi, X., Bakht, S., Leggett, M., Maxwell, C., Melton, R., and Osbourn, A. (2004). A gene cluster for secondary metabolism in oat: Implications for the evolution of metabolic diversity in plants. Proc. Natl. Acad. Sci. USA **101:** 8233–8238.

Qi, X., Bakht, S., Qin, B., Leggett, M., Hemmings, A., Mellon, F., Eagles, J., Werck-Reichhart, D., Schaller, H., Lesot, A., Melton, R., and Osbourn, A. (2006). A different function for a member of an ancient and highly conserved cytochrome P450 family: From essential sterols to plant defense. Proc. Natl. Acad. Sci. USA **103:** 18848–18853.

Qin, B., Eagles, J., Mellon, F.A., Mylona, P., Peña-Rodriguez, L.M., and Osbourn, A.E. (2010). High throughput screening of mutants of oat that are defective in triterpene synthesis. Phytochemistry **71:** 1245–1252.

Radwanski, E.R., and Last, R.L. (1995). Tryptophan biosynthesis and metabolism: Biochemical and molecular genetics. Plant Cell **7:** 921–934.

Rohde, B., Hans, J., Martens, S., Baumert, A., Hunziker, P., and Matern, U. (2008). Anthranilate *N*-methyltransferase, a branch-point enzyme of acridone biosynthesis. Plant J. **53:** 541–553.

Ruelland, E., Campalans, A., Selman-Housein, G., and Puigdomènech, J., and Rigaul, J. (2003). Cellular and subcellular localization of the lignin biosynthetic enzymes caffeic acid-*O*-methyltransferase, cinnamyl alcohol dehydrogenase and cinnamoyl-coenzyme A reductase in two monocots, sugarcane and maize. Physiol. Plant. **117:** 93–99.

Sainsbury, F., Lavoie, P.-O., D'Aoust, M.-A., Vézina, L.-P., and Lomonossoff, G.P. (2008). Expression of multiple proteins using full-length and deleted versions of cowpea mosaic virus RNA-2. Plant Biotechnol. J. **6:** 82–92.

Schmid, J., and Amrhein, N. (1995). Molecular organization of the shikimate pathway in higher plants. Phytochemistry **39:** 737–749.

Shimura, K., et al. (2007). Identification of a biosynthetic gene cluster in rice for momilactones. J. Biol. Chem. **282:** 34013–34018.

Shirley, A.M., and Chapple, C. (2003). Biochemical characterization of sinapoylglucose:choline sinapoyltransferase, a serine carboxypeptidase-like protein that functions as an acyltransferase in plant secondary metabolism. J. Biol. Chem. **278:** 19870–19877.

Shirley, A.M., McMichael, C.M., and Chapple, C. (2001). The *sng2* mutant of *Arabidopsis* is defective in the gene encoding the serine carboxypeptidase-like protein sinapoylglucose:choline sinapoyltransferase. Plant J. **28:** 83–94.

Simpson, C., Thomas, C., Findlay, K., Bayer, E., and Maule, A.J. (2009). An *Arabidopsis* GPI-anchor plasmodesmal neck protein with callose binding activity and potential to regulate cell-to-cell trafficking. Plant Cell **21:** 581–594.

Stehle, F., Stubbs, M.T., Strack, D., and Milkowski, C. (2008). Heterologous expression of a serine carboxypeptidase-like acyltransferase and characterization of the kinetic mechanism. FEBS J. **275:** 775–787.

St-Pierre, B., Laflamme, P., Alarco, A.M., and De Luca, V. (1998). The terminal *O*-acetyltransferase involved in vindoline biosynthesis defines a new class of proteins responsible for coenzyme A-dependent acyl transfer. Plant J. **14:** 703–713.

Swaminathan, S., Morrone, D., Wang, Q., Fulton, D.B., and Peters, R.J. (2009). CYP76M7 is an ent-cassadiene C11alpha-hydroxylase defining a second multifunctional diterpenoid biosynthetic gene cluster in rice. Plant Cell **21:** 3315–3325.

Takos, A.M., Knudsen, C., Lai, D., Kannangara, R., Mikkelsen, L., Motawia, M.S., Olsen, C.E., Sato, S., Tabata, S., Jørgensen, K., Møller, B.L., and Rook, F. (2011). Genomic clustering of cyanogenic glucoside biosynthetic genes aids their identification in *Lotus japonicus* and suggests the repeated evolution of this chemical defence pathway. Plant J. **68:** 273–286.

Takos, A.M., and Rook, F. (2012). Why biosynthetic genes for chemical defense compounds cluster. Trends Plant Sci. **17:** 383–388.

Tamura, K., Dudley, J., Nei, M., and Kumar, S. (2007). MEGA4: Molecular evolutionary genetics analysis (MEGA) software version 4.0. Mol. Biol. Evol. **24:** 1596–1599.

Walker, K., Long, R., and Croteau, R. (2002). The final acylation step in taxol biosynthesis: Cloning of the taxoid C13-side-chain *N*-benzoyltransferase from *Taxus*. Proc. Natl. Acad. Sci. USA **99:** 9166–9171.

Wang, J., and Pichersky, E. (1999). Identification of specific residues involved in substrate discrimination in two plant *O*-methyltransferases. Arch. Biochem. Biophys. **368:** 172–180.

Wilderman, P.R., Xu, M., Jin, Y., Coates, R.M., and Peters, R.J. (2004). Identification of *syn*-pimara-7,15-diene synthase reveals functional clustering of terpene synthases involved in rice phytoalexin/allelochemical biosynthesis. Plant Physiol. **135:** 2098–2105.

Wegel, E., Koumproglou, R., Shaw, P., and Osbourn, A. (2009). Cell type-specific chromatin decondensation of a metabolic gene cluster in oats. Plant Cell **21:** 3926–3936.

Weier, D., Mittasch, J., Strack, D., and Milkowski, C. (2008). The genes *BnSCT1* and *BnSCT2* from *Brassica napus* encoding the final enzyme of sinapine biosynthesis: Molecular characterization and suppression. Planta **227:** 375–385.

Winzer, T., et al. (2012). A *Papaver somniferum* 10-gene cluster for synthesis of the anticancer alkaloid noscapine. Science **336:** 1704–1708.

Yang, Q., Reinhard, K., Schiltz, E., and Matern, U. (1997). Characterization and heterologous expression of hydroxycinnamoyl/benzoyl-CoA:anthranilate N-hydroxycinnamoyl/benzoyltransferase from elicited cell cultures of carnation, *Dianthus caryophyllus* L. Plant Mol. Biol. **35:** 777–789.

Yazaki, K., Inushima, K., Kataoka, M., and Tabata, M. (1995). Intracellular localization of UDPG:*p*-hydroxybenzoate glucosyltransferase and its reaction product in *Lithospermum* cell cultures. Phytochemistry **38:** 1127–1130.

Yu, X.-H., Chen, M.-H., and Liu, C.-J. (2008). Nucleocytoplasmic-localized acyltransferases catalyze the malonylation of 7-O-glycosidic (iso)flavones in *Medicago truncatula*. Plant J. **55:** 382–396.